Macedonian Journal of Chemistry and Chemical Engineering, Vol. **35**, No. 1, pp. 97–105 (2016)

MJCCA9 – 708

ISSN 1857-5552
e-ISSN 1857-5625

Received: December 23, 2015
Accepted: March 17, 2016

UDC:549.67:543.422.3-74
DOI:10.20450/mjcce.2016.850
Original scientific paper

LOW-TEMPERATURE PLASMA-MODIFIED ZEOLITE VS. NATURAL BULGARIAN ZEOLITE – COMPARATIVE PHYSICOCHEMICAL, SPECTROPHOTOCHEMICAL AND FOURIER TRANSFORM INFRARED SPECTROSCOPY STUDIES

Zvezdelina Yaneva*, Nedyalka Georgieva, Angel Pavlov

Chemistry Unit, Department of Pharmacology, Animal Physiology and Physiological Chemistry, Faculty of Veterinary Medicine, Trakia University, Students Campus, 6000 Stara Zagora, Bulgaria

*z.yaneva@abv.bg

In this study, we investigate and compare the physicochemical and morphological properties, as well as the sorption potential, of a natural Bulgarian zeolite (NBZ) and a low-temperature plasma-modified zeolite (LTPMZ). The NBZ was treated with low-temperature arc plasma. The evolution of the modifications was followed using Fourier transform infrared spectroscopy (FTIR), ultraviolet-visible spectrophotometric (UV-VIS), physicochemical and sorption studies. Digital microscope analyses proved that the crystallinity, sheet structure and textural properties of the natural material were not significantly affected by the plasma treatment. The comparative analyses of the obtained FTIR spectra showed that the plasma treatment caused the breakdown of siloxane groups at the clay surface and induced the formation of new silanol groups at the clay edges. According to the UV/VIS and FTIR studies of Rhodamine 6G (Rh6G) sorption, the LTPMZ displayed a higher affinity to the cationic dye compared to the NBZ. This study demonstrates that low-temperature plasma treatments could be used to activate zeolites for environmental applications.

Keywords*:* natural zeolite; low-temperature arc plasma; FTIR; UV/VIS; Rhodamine 6G

НИСКОТЕМПЕРАТУРЕН ЗЕОЛИТ МОДИФИЦИРАН СО ПЛАЗМА СПОРЕДЕН СО БУГАРСКИ ЗЕОЛИТ – КОМПАРАТИВНИ ФИЗИЧКО-ХЕМИСКИ, СПЕКТРОХЕМИСКИ И ФУРИЕ-ТРАНСФОРМНИ ИНФРАЦРВЕНИ СПЕКТРОСКОПСКИ ИСПИТУВАЊА

Во оваа студија ги испитувавме и ги споредивме физичко-хемиските и морфолошките својства, како и сорпциониот потенцијал на природниот бугарски зеолит (NBZ) и нискотемпературниот зеолит модифициран со плазма (LTPMZ). NBZ беше третиран во нискотемпературен лак. Еволуцијата на модификациите беше следена со примена на Фуриеова трансформна инфрацрвена спектроскопија (FTIR), видлива ултравиолетова спекторметрија (UV-VIS), како и преку физичко-хемиски и сорпцисики испитувања. Дигиталната микроскопска анализа покажа дека кристалните својства, структурата на слоевите и својствата на текстурата на природниот материјал значајно не се менуваат при обработката со плазма. Компаративната анализа на FTIR-спектрите покажува дека третманот со плазма предизвикува раскинување на силоксанските групи на површината на глината и индуцира образување на нови силанолни групи на рабовите на глината. Според испитувањата со UV-VIS и FTIR на сорпцијата на родамин 6G (Rh6G), LTPMZ има повисок афинитет кон катјонски бои во споредба со NBZ. Ова истражување покажува дека нискотемпературната обработка со плазма може да се примени за активирање на зеолити кои се користат во еколошки цели.

Клучни зборови*:* природен зеолит; нискотемпературна плазма со лак; FTIR; UV/VIS; Rhodamine 6G1

INTRODUCTION

Many advances have recently been made in the development of surface treatments for altering the chemical and physical properties of material surfaces without affecting the bulk properties. Common surface modification techniques include flame, corona, plasma, photon, electron beam, ion beam, X-ray and γ-ray treatments [1].

In addition to being environmentally friendly, plasma treatment is probably the most versatile surface treatment technique. The different species present in the plasma induce the formation of free radicals and, thus, it is possible to insert or interlock certain functional groups on material surfaces [1].

The importance and widespread use of zeolites are due to the versatility of their properties, as well as the fact, that in general, they are environmentally friendly substances. New standards and challenges require constant improvement of the known materials and the discovery of new microporous zeolite type materials [2].

Low-temperature plasmas, including thermal and nonthermal plasmas, are extremely important for the synthesis and processing of materials [3]. Based upon the mechanism of how plasma is generated, the pressure applied and the electrode geometry, nonthermal plasmas can have several very different types, including glow discharge, silent discharge (or dielectric barrier discharge) and RF discharge [3, 4].

Our scientific team previously studied the equilibrium behavior of 4-nitrophenol during its adsorption on Romanian and Bulgarian zeolites from aqueous solutions [5], as well the host-guest interactions during caffeine encapsulation into a natural Bulgarian zeolite (NBZ) [6].

The present research presents an innovative environmentally friendly technique for natural zeolite modification by low temperature plasma treatment, inspired by the lack of such investigations in the literature.

The aim of the current study is to investigate and compare the physicochemical and morphological properties, as well as the sorption potential, of a NBZ and a low-temperature plasma modified zeolite (LTPMZ), and to assess their possible applications as low-cost environmentally friendly adsorbents for cationic organic species removal from water.

2. EXPERIMENTAL

2.1. *Natural zeolite*

The natural zeolite used in the present study was supplied by Bentonite AD, Kurdzhali City, Bulgaria. Its basic physicochemical properties are listed in Table 1. The theoretical total ion exchange capacity is 2.05 meq g^{-1} and the Si/Al ratio is 6.01 [7].

T a b l e 1

Physicochemical properties of the natural zeolite

Pore volume, $cm^3\ g^{-1}$	0.11
Density, $g\ cm^{-3}$	1.10
Specific surface area, $m^2\ g^{-1}$	37.1
pH	6.9-7.0
Clinoptilolite content, %	87 %

Prior to the sorption experiments, the mineral composite was thoroughly washed several times with distilled water to remove dust and any adhering substances. The washed material was oven dried at 373 K for 48 h. The prepared samples were stored in airtight containers for further studies. The fraction used was 0.5–3.0 mm.

2.2. *Cationic fluorescent dye*

Rhodamine 6G (Rh6G, Basic Red I) (C.I. 45160) is a cationic fluorescent azo dye with molecular formula $C_{28}H_{31}N_2O_3Cl$ (Fig. 1), and was obtained from Sigma-Aldrich. Dye concentrations were determined spectrophotometrically at 526 nm.

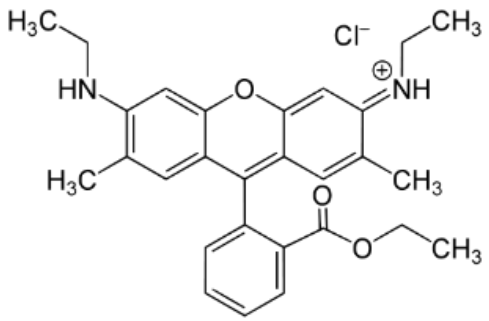

Fig. 1. Molecular structure of Rh6G

2.3. *Instrumentation for the plasma discharge*

Plasma Pen PVA TePla AG (PVA TePLa AG, USA) was used for modification of the NBZ. The plasma pen produces high-density plasma with a low heating effect, giving it the ability to clean and activate surfaces. The plasma pen was an arc discharge type, with a power of 100 W, tested gas mixtures of compressed air and O_2 and a gas flow of 1275 $dm^3\ h^{-1}$. The scheme of the experimental setup is presented in Figure 2.

The fresh and Rhodamine 6G-loaded natural zeolite samples were treated with air for 2 min at T = 108–110 °C.

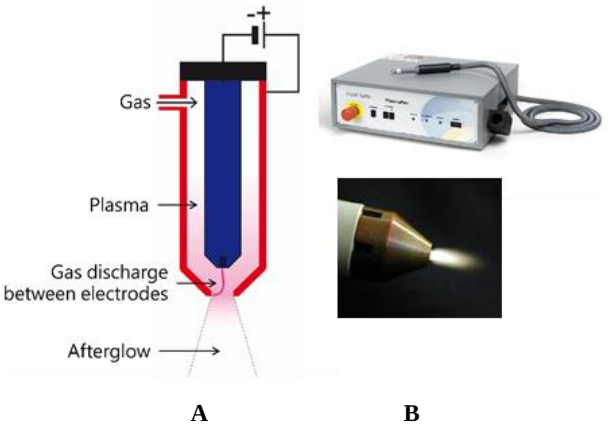

Fig. 2. Scheme of the experimental setup:
A) Arc discharge torch. **B**) Plasma pen

2.4. *Characterization of the NBZ and LTPMZ*

The surface chemistry of the zeolites was characterized by Boehm titration, the pH of zero charge, FTIR and digital microscope analysis.

The acidic and basic sites on the NBZ and LTPMZ were determined by the acid-base titration (potentiometric titration) method proposed by Boehm [8, 9]. The total acidic sites were neutralized using NaOH (0.1 mol dm^{-3}), while the basic sites were neutralized with HCl (0.1 mol dm^{-3}). The potentiometric titration curves were obtained by plotting the volume of titrant against the recorded pH.

The zero surface charge (pH_{PZC}) characteristics of the NBZ and LTPMZ were determined using the solid addition method [9]. A 0.1 mol dm^{-3} NaCl solution (40 cm^3) was transferred to a series of 250 cm^3 stoppered conical flasks. The pH_i values of the solutions were adjusted between 2 and 11 by adding either 0.1 mol dm^{-3} HCl or 0.1 mol dm^{-3} NaOH. The total volume of the solution in each flask was exactly adjusted to 50 cm^3 by adding NaCl solution of the same strength. The pH_i of the solutions were then accurately noted.

NBZ/LTPMZ (0.5 g) was added to each flask, and the flasks were securely capped immediately. The suspensions were then kept shaking for 24 h and allowed to equilibrate for 0.5 h. The final pH values of the supernatant liquids were noted. The difference between the initial and final pH (pH_f) values (ΔpH) was plotted against pH_i. The point of intersection of the resulting curve with abscissa, at which the pH equals zero, gave the pH_{PZC}.

The microscope morphological analyses of the NBZ before and after plasma modification and dye sorption were conducted with a digital microscope at 500× magnification. The pH was measured on a pH-meter, Consort C931, Belgium.

FTIR spectra of the fresh NBZ, fresh LTPMZ, dye-loaded NBZ and dye-loaded LTPMZ were obtained with the KBr disc technique in the range of 400-4000 cm^{-1} using a TENSOR 37 Bruker FTIR spectrometer (Bruker Optik GmbH, Germany).

2.5. *Sorption studies*

To assess and compare the sorption potential of the NBZ and LTPMZ, the cationic dye Rhodamine 6G was applied as a sorbate.

The sorption experiments were carried out by agitating a predetermined mass of natural zeolite (1 g) with 50 cm^3 of Rh6G solutions with initial concentrations of c_0 = 5–35 mg dm^{-3} at a temperature, T, of 19±2 °C and pH values of 7.5 and 8.0 for experiments with the NBZ and LTPMZ, respectively. The sorbate/sorbent systems were agitated on an IKA®KS 130 basic shaker at 180 rpm until equilibrium was reached. Then, the dye solutions were separated from the adsorbent by centrifugation with a Heraeus Labofuge 200 (Thermo, Electron Corporation) at 5300 g for 20 min and filtered using 0.45 μm membrane filters (LCW 916, Hach Lange, Germany) to ensure the solutions were free from adsorbent particles before subsequent FTIR analyses to measure the residual dye concentration.

Rhodamine 6G concentrations were measured by a UV/VIS spectrophotometer DR 5000 (Hach Lange, Germany) supplied with 10 mm quartz cells. All spectra were recorded in the VIS region at λ = 526 nm with a 2 nm slit width, a 900 nm min^{-1} scan speed and very high smoothing.

The experimental equilibrium sorption capacity (q_e) of the NBZ and LTPMZ was calculated by the following mass balance equation:

$$(c_o - c_e)\cdot V = (q_e - q_o)\cdot w, \qquad (1)$$

where c_o is the initial dye concentration in the liquid phase in mg dm^{-3}, q_o = 0 and w is the sorbent mass in g.

3. RESULTS AND DISCUSSION

3.1. *Potentiometric titration*

The acidic and basic sites and functional groups present on the NBZ and LTPMZ were determined by potentiometric titration. In order to gain a better insight into the surface properties of the minerals, for acidic sites, zeolite suspension in 0.1 mol dm^{-3} HCl was potentiometrically titrated

with 0.1 mol dm^{-3} NaOH. Likewise, the NaOH suspensions of both zeolites were potentiometrically titrated with 0.1 mol dm^{-3} HCl for determination of the basic sites and the respective curves are presented in Figure 3.

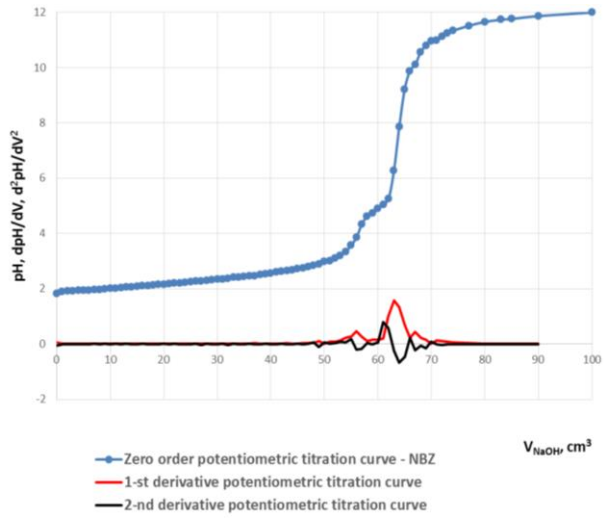

A

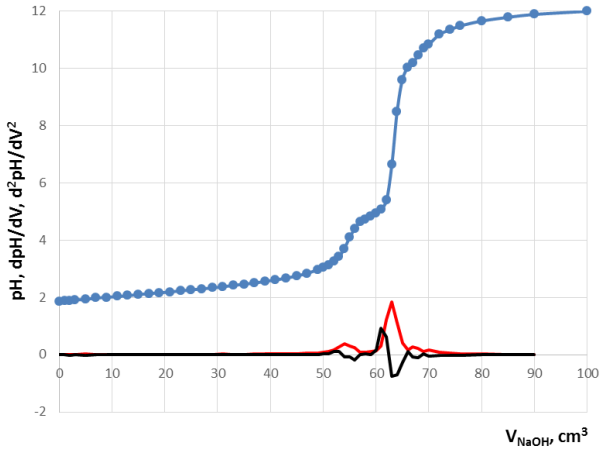

B

Fig. 3. Zero order, first and second derivative potentiometric titration curves of NBZ **(A)** and LTPMZ **(B)**

Both titration curves displayed four inflexion points and the corresponding pK_a values suggested the binding functional groups were present on the zeolite surface. The results of the titration permitted the qualitative and semi-quantitative determination of the nature and number of active (acidic, basic) sites present. The curve in Figure 3 showed four flexion points at approximately pH 6.64 corresponding to pK_a values of 6.64 and 3.71. According to the experimental data, the basic and acidic sites for the NBZ were estimated to be 2.5 and 6.3 mmol g^{-1}, respectively, and for the LTPMZ, 3.3 and 6.3 mmol g^{-1}, respectively. Thus, the observed higher concentration of acidic sites, compared to that of the basic ones, determined the acidic surface of both mineral materials. The observed higher concentration of basic sites on the surface of the LTPMZ could be attributed to the formation of new hydroxyl groups (Si–OH and Al–OH) on the clay edges induced by the plasma treatment.

It is observed from Figure 4 that the surface charge of the NBZ is zero at pH 7.35, and that of LTPMZ is zero at pH 7.5. Hence, the pH_{PZC} values of NBZ and LTPMZ are 7.35 and 7.5, respectively.

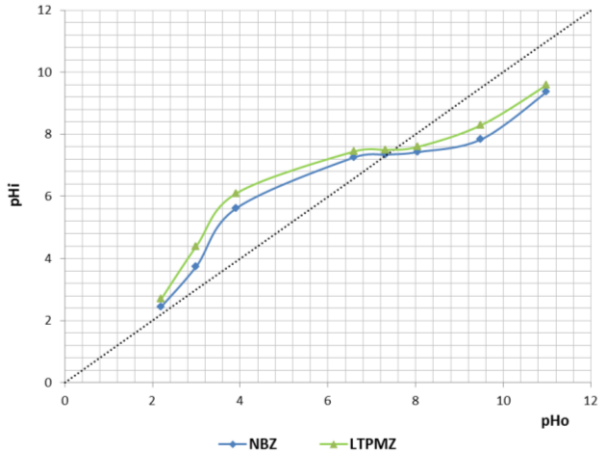

Fig. 4. pH_{pzc} of NBZ and LTPMZ

3.2. *UV-VIS spectrophotometric analyses*

The UV/VIS spectra of Rh6G at λ = 526 nm before and after sorption on the natural zeolite are presented in Figure 5.

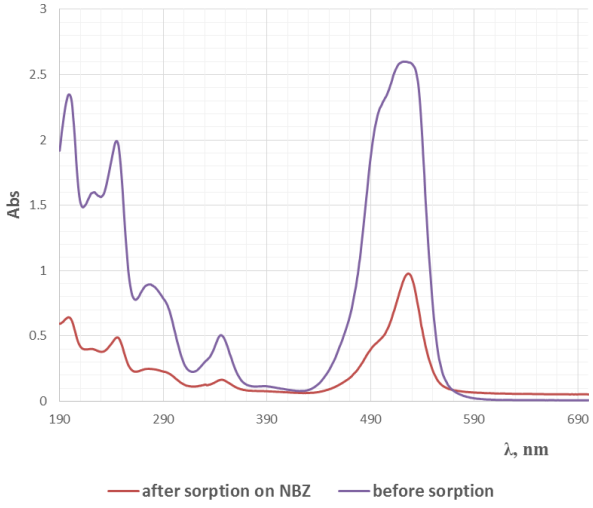

Fig. 5. UV/VIS spectra of Rh6G before and after sorption onto NBZ (λ = 526 nm)

Obviously, the intensity of the peak after adsorption decreased. The uptake efficiency was estimated to E 39 %. However, the maximum dye absorbance did not change. In addition, the modes of both peaks were approximately identical. Consequently, the process of Rh6G adsorption on zeolite did not affect the structure of the dye molecules.

3.3. *Zeolite morphology*

The digital microscope images of the NBZ and LTPMZ and Rh6G-loaded zeolite, presented in Figs. 6 A, B and C, respectively, display the heterogeneity of the three samples and the irregular distribution of the dye macromolecules on irregular regions of the solid particles surface.

A

B

C

Fig. 6. Digital microscope images (500×) of: **A**) NBZ, **B**) LTPMZ and **C**) Rh6G-LTPMZ

3.4. *Equilibrium sorption of Rh6G on the NBZ and LTPMZ*

During the equilibrium sorption studies, it was established that the maximum experimental equilibrium capacity of NBZ towards Rh6G was q_{max} 2.23 mg g^{-1}, while that of LTPMZ was approximately 1.3 times higher, q_{max} 2.9 mg g^{-1}. Both studied systems reached equilibrium in 24 h. The experimental equilibrium data is presented in Figure 7. Obviously, the initial rate of the dye sorption on the modified zeolite was significantly higher, as denoted by the steep slope of the experimental isotherm in the low concentration range. After that, the modes of both isotherms were similar.

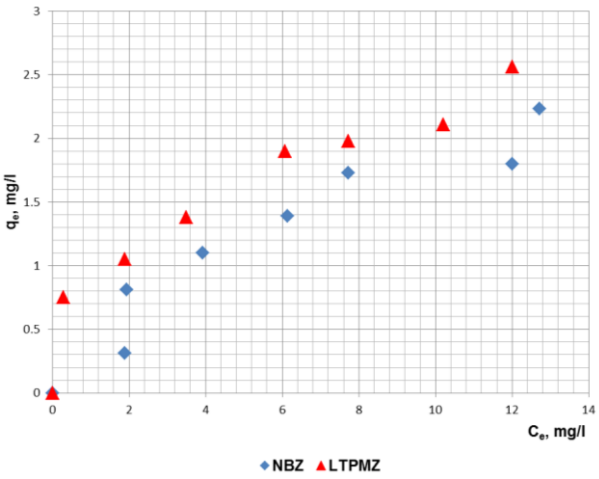

Fig. 7. Experimental equilibrium isotherms of Rh6G sorption on NBZ and LTPMZ

3.5. *FTIR analyses*

FTIR analyses were conducted to identify the locations of functional groups in the NBZ and their modification in the LTPMZ, as well as possible interactions between functional groups of Rh6G molecules and the NBZ before and after plasma modification.

3.5.1. *Comparative assignment of FTIR bands of fresh NBZ and LTPMZ*

The FTIR spectra of fresh NBZ and LTPMZ, measured within the range 4000-400 cm^{-1}, are presented in Figure 8. Generally, the bands at ~3620 cm^{-1} correspond to stretching vibrations of structural OH-groups, particularly lattice terminal silanol groups. Those at 3460–3440 cm^{-1} and ~1640 cm^{-1} are assigned to stretching vibrations and deformation of adsorbed water, respectively. The most intense bands around 1050 cm^{-1} are attributed to stretching vibrations of Si-O bonds in the tetrahedral layer, while those at ~505 and 470 cm^{-1} are due to the deformation of Si-O-Al (Al as octahedral cation) and Si-O-Si, respectively. The peak at 795 cm^{-1} is attributed by some researchers to the vibration of Si-O bonds in quartz impurities.

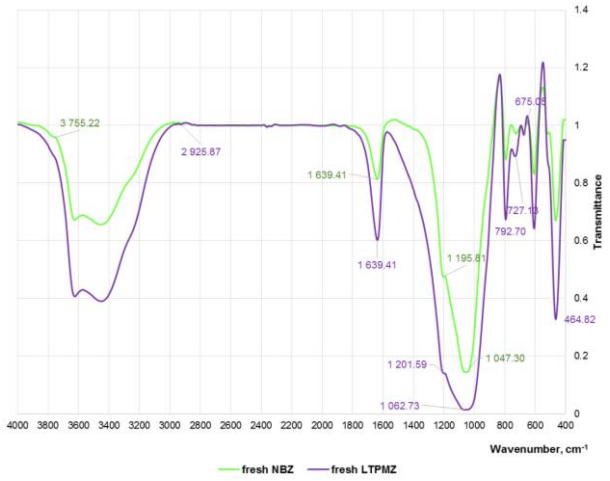

Fig. 8. Comparative FTIR spectra of fresh NBZ and LTPMZ

The comparative analyses of the FTIR spectra of NBZ and LTPMZ, however, displayed variations in the intensity of the relevant bands (Fig. 8). The first type of OH-groups present in the NBZ, the lattice termination silanol groups (~3750 cm^{-1}), are located on the external surface of the mineral particles. Obviously, they are not characteristic of the plasma-modified samples as the relevant FTIR band is missing. The bands attributed to the bridging OH-groups with Bronsted acidity (~3620 cm^{-1} and 3460–3440 cm^{-1}) on the FTIR spectra of the LTPMZ are more resolved and characterized with greater area, which is an indication of their increased number (Fig. 8).

This latter point is further proof that the low-temperature plasma treatment causes the breakdown of siloxane bonds, which induces the formation of local silanol effects.

The band at 2925 cm^{-1}, registered only in the FTIR spectra of the LTPMZ, belongs to overtone harmonic in-plane bending vibrations of H-O-H [10]. The medium intensity band of the H-O-H vibrations in the region 1630–1640 cm^{-1} in the LTPMZ spectra occurs at lower transmittance. The position of the peak at ~465 cm^{-1} is maintained in both spectra. There is a slight shift of the absorption bands at 796 cm^{-1} (for the NBZ) to 792 cm^{-1} (for the LTPMZ) with a significant increase in the intensity of the LTPMZ spectrum. This gives evidence of the alteration of sample crystallinity after the plasma modification.

According to the spectral data, the low-temperature plasma modification lead to dealumination of the mineral samples, accompanied by the rupture of Si-O-Al bonds, as the resulting shift of asymmetric valent intra-tetrahedral vibrations frequency moved to the higher wavelength region, from 1047 to 1062 cm^{-1}. In addition, the latter spectral band was characterized with a greater area. Most of the octahedral sites were occupied by divalent central atoms, thus the O–H bending bands were shifted to wavenumbers in the 700–600 cm^{-1} range [11].

3.5.2. *Comparative assignment of FTIR bands of Rh6G-loaded NBZ and LTPMZ*

The incorporation of the cationic dye in the NBZ and LTPMZ displayed variations in the intensity of relevant bands on the FTIR spectra of both Rh6G-loaded minerals (Table 2; Figs. 9 and 10).

In addition to the strong bands caused by the host zeolite, the FTIR spectra of the Rh6G-loaded NBZ displayed split bands in the region of 2923−2854 cm^{-1} (Fig. 9), these are assigned to OH-stretching vibrations, as well as aliphatic C-H stretching vibrations of the adsorbed dye molecules.

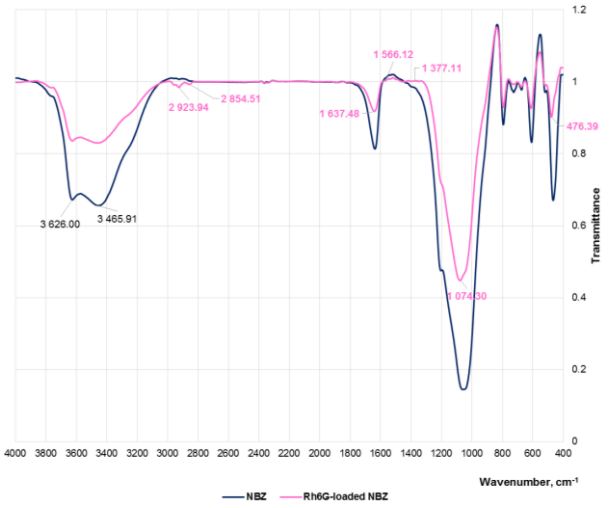

Fig. 9. Comparative FTIR spectra of fresh NBZ and Rh6G-loaded NBZ

The small bands in the regions of 2360–2218 and 1585–1377 cm^{-1}, registered in the spectra of both dye-loaded minerals, supported the presence of Rh6G molecules and were attributed to NH-, C=N-stretching vibrations and C=O stretching of the organic molecules, respectively.

The higher extent of Rh6G sorption by the LTPMZ, compared to the NBZ, was proven by the observed segmentation of the band in the region of 1200–1000 cm^{-1}, accompanied by the appearance of a weak band at 1089 cm^{-1}, characteristic of aromatic ring vibrations (ν_{ring}) (Fig. 10).

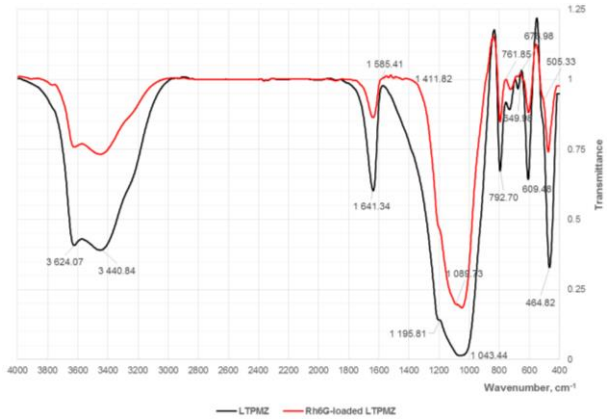

Fig. 10. Comparative FTIR spectra of fresh LTPMZ and Rh6G-loaded LTPMZ

Furthermore, the well-resolved fluctuations in the spectra at 761 cm^{-1}, in the region of 700-600 cm^{-1} and at 505 cm^{-1} were assigned to CH- plane and out-of-plane deformations, -C≡C and C-C=O band vibrations, respectively (Table 2).

Although for both studied Rh6G-loaded zeolite systems, the FTIR spectra were dominated by the strong bands assigned to the vibration of the zeolites structures, the characteristic Rh6G FTIR vibrational bands were well resolved, especially in the spectra of the Rh6G-loaded LTPMZ, they provided significant evidence for the presence of the dye molecules in the zeolite matrices.

T a b l e 2

Characteristic bands on the FTIR spectra of Rh6G-loaded NBZ and fresh LTPMZ

υ (cm^{-1})	**Vibrations**		
	Rh6G-loaded NBZ	**Rh6G-loaded LTPMZ**	**Rh6G** [12]
3626	Lattice termination silanol groups		
3624		Lattice termination silanol groups	
3465	Symmetric stretching vibration of H_2O		
3440		Symmetric stretching vibration of H_2O	
2923–2854	OH-stretching*, aliphatic C-H vibrations*		OH-stretching, aliphatic C-H vibrations
2360–2218	NH-stretching*, C=N-stretching*	NH-stretching*, C=N-stretching*	NH-stretching, C=N-stretching
1639	Bending vibration of H_2O	Bending vibration of H_2O	
1585–1377	C=O stretching*	C=O streching*	C=O streching
1195	Internal tetrahedra asymmetric stretching vibrations		
1201		Internal tetrahedra asymmetric stretching vibrations	
1089		**ν_{ring}***	ν_{ring}
1045	Si–O stretching mode of aluminosilicates, Al(III) in the octahedral position		
1043		Si–O stretching mode of aluminosilicates, Al(III) in the octahedral position	
796	Internal tetrahedra symmetric stretching vibrations		
792		Internal tetrahedra symmetric stretching vibrations	
761		**CH out of plane deformation***	CH out of plane deformation
700–600	Octahedral sites occupied by divalent central atoms	Octahedral sites occupied by divalent central atoms; **CH of plane*; -C≡C band***	CH of plane, -C≡C band
505		**C-C=O band***	C-C=O band
466	O-T-O bending vibration		
464		O-T-O bending vibration	

*FTIR vibrations attributed to Rh6G molecules.

3.6. *Sorption mechanism*

The sorption mechanism of Rh6G in both zeolite materials was analyzed by the dye molecule stereochemistry and by the probable variations of the zeolite framework and molecular characteristics in the process of its plasma modification.

π-Interactions between the oxygen planes of the clay and the aromatic rings of the organic dye cannot occur in R6G due to steric hindrance, in this molecule the phenyl ring is sterically constrained to be roughly perpendicular to the planar xanthene group [13].

In order to verify the hypothesis of electrostatic adsorption, the zeta potential was applied to investigate charge type of materials surface, charge quantity and its stability in different pH solutions. The isoelectric point of NBZ is observed at pH 7.35 and of LTPMZ at pH 7.5. Above this pH values, the natural and modified zeolite particles are negative in aqueous solutions and they can capture positive cationic dyes like Rh6G in theory. Thus, the equilibrium sorption experiments with NBZ were conducted at pH 7.5 and these with LTPMZ at pH 8. Thus, as Rh6G is a cationic dye, it can be adsorbed easily by electrostatic forces on negatively charged surfaces.

Alternatively, one can expect that the hydrophobic interaction between the surface of zeolite and the ester group (–$COOCH_3$) in Rh6G molecules might take place in the adsorption process as well, which would facilitate the efficient uptake on the mineral surface adsorbent. Therefore, on the basis of the electrostatic and inter-molecular interactions, it can be preliminarily concluded that the much higher adsorption capacity of Rh6G should be caused by the hydrophobic interaction forces from the ester group (–$COOCH_3$) in Rh6G molecules (Fig. 11).

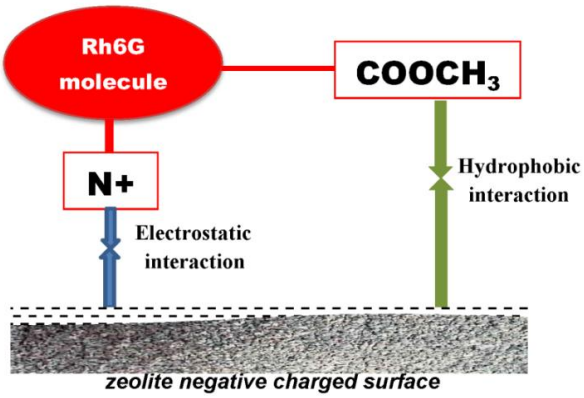

Fig. 11. Illustration of the electrostatic/hydrophobic interactions between Rh6G molecules and a zeolite surface

The FTIR analyses of the fresh NBZ and LTPMZ proved the breakdown of siloxane bonds, which induces the formation of local silanol effects [14]. The nature of these effects, however, could be different. The silanol groups can be isolated (free silanol groups), where the surface silicon atom has three bonds into the bulk structure and the fourth to OH-group and the vicinal or bridged silanols, where two isolated silanol groups attached to two different silicon atoms are bridged by H-bond. A third type of silanols, called geminal silanols, consist of two hydroxyl groups attached to one silicon atom [15]. Geminal silanols are close enough to have H-bonds, whereas free silanols are too far apart, as indicated in Figure 12.

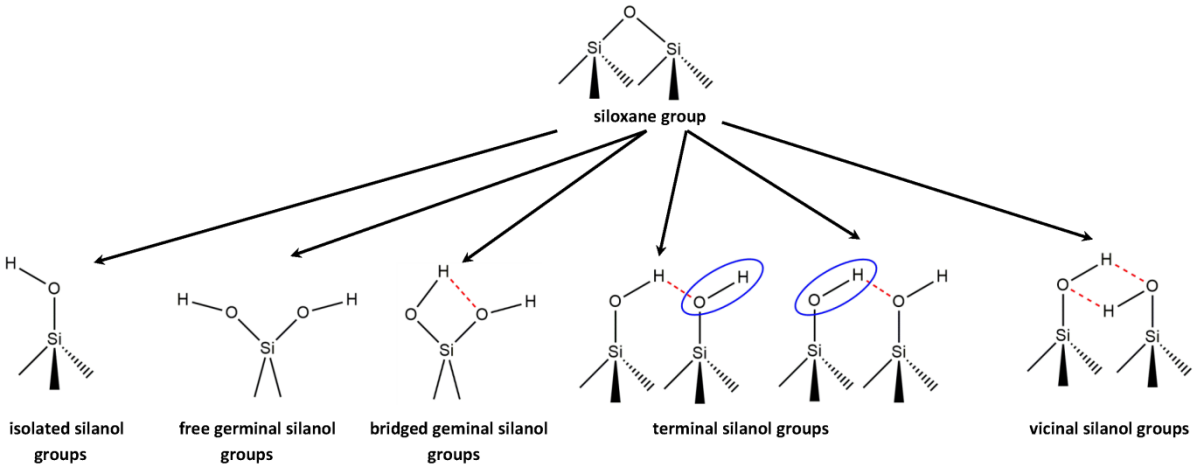

Fig. 12. Types of silanol groups formed on the LTPMZ surface after low-temperature plasma modification

Consequently, the defects in the microporosity of the zeolite, formed as a result of the low-temperature plasma treatment, led to the formation of a greater number of germinal, terminal and/or vicinal silanols on the mineral surface. Thus, the formation of H-bonds between them led to "neutralization" of their basicity and the decrease of the hindering effect of the silanol groups towards the realization of hydrophobic interactions.

4. CONCLUSIONS

The surface modifications occurring during low-temperature plasma treatment of natural Bulgarian zeolite were evaluated using FTIR spectroscopy, UV/VIS spectrophotometry, potentiometric titration, digital microscopy and sorption studies. The comparative analyses of the experimental results in the present study established that the reactive species created in low-temperature plasma medium were able to break down the siloxane bounds of the zeolite edges to form various silanol groups. The sorption capacity of the LTPMZ towards Rh6G was increased, probably due to the formation of H-bonds between the germinal, terminal and/or vicinal silanols, leading to the decrease of the hindering effect of the silanol groups towards the realization of hydrophobic cationic dye/LTPMZ surface interactions. Future studies will be directed to investigations on the potential of LTPMZ to adsorb anionic dyes, as their affinity to the LTPMZ is likely to be significantly higher compared to NBZ, as well as being biologically active substances.

Acknowledgements. The study was supported financially by Scientific Project No. 14–15 VMF, Faculty of Veterinary Medicine, Trakia University, Stara Zagora, Bulgaria.

REFERENCES

[1] K. Fatyeyeva, F. Poncin-Epaillard, Sulfur dioxide plasma treatment of the clay (laponite) particles plasma, *Chem Plasma Process*, **31**, 449–464 (2011). DOI: 10.1007/s11090-011-9291-6

[2] M. El-Roz, L. Lakiss, A. Vicente, K. N. Bozhilov, F. Thibault-Starzyk, V. Valtchev, Ultra-fast framework stabilization of Ge-rich zeolites by low-temperature plasma treatment, *Chemical Science*, **5** (1), 1–428 (2014). DOI:10.1039/C3SC51892B

[3] A. Tiya Djowe, S. Laminsi, D. Njopwouo, E. Acayanka, E. M. Gaigneaux, Surface modification of smectite clay induced by non-thermal gliding arc plasma at atmospheric pressure, *Plasma Chem. Plasma. Process* (2013). DOI:10.1007/s11090-013-9454-8.

[4] C. Liu, J. Zou, K. Yu, D. Cheng, Y. Han, J. Zhan, C. Ratanatawanate, B. W.-L. Jang, Plasma application for more environmentally friendly catalyst preparation, *Pure Appl. Chem*., **78** (6), 1227–1238 (2006). DOI: 10.1351/pac200678061227

[5] Z. Kircheva-Yaneva, G. Oltean, D. Covaciu, B. Koumanova, M. Zitaru, Equilibrium study of 4-nitrophenol adsorption on natural materials from aqueous solutions. *J. Univ. Chem. Technol. Met. (Sofia)*, **39** (3), 343–350 (2004).

[6] Z. Yaneva, M. Staleva, N. Georgieva, Study on the host-guest interactions during caffeine encapsulation into zeolite, *European Journal of Chemistry*, **6** (2), 169–173 (2015). DOI: dx.doi.org/10.5155/eurjchem.6.2.169-173.1228

[7] E. Ivanova, M. Karsheva, B. Koumanova, Adsorption of ammonium ions onto natural zeolite, *J. Univ. Chem. Technol. Met. (Sofia)*, **45** (3), 295–302 (2010).

[8] H. P. Boehm, Some aspects of the surface chemistry of carbon blacks and other carbons, *Carbon*, **32**, 759–769 (1994). DOI:10.1016/0008-6223(94)90031-0

[9] B. H. Hameed, Evaluation of papaya seed as a novel non-conventional low-cost adsorbent for removal of methylene blue, *J. Hazard. Mater*., **162**, 939–994 (2010). DOI: 10.1016/j.jhazmat.2008.05.120

[10] F. Pechar, D. Rykl, Infrared spectra of natural zeolites of the stilbite group, *Chem. Zvesti*, **35** (2), 189–202 (1981).

[11] B. Stuart, *Infrared Spectroscopy: Fundamentals and Applications*, John Wiley & Sons, West Sussex PO19 8SQ, England, 2004.

[12] S. Bakkialakshmi, T. Menaka, A detailed spectroscopic study on the interaction of Rhodamine 6G with two amines, *International Journal of Current Research*, **10**, 021–024 (2010).

[13] M. J. Tapia Estevez, F. Lopez Arbeloa, T. Lopez Arbeloa, I. Lopez Arbeloa, R. A. Schoonheydt, Adsorption of rhodamine 6G on laponite B for low loadings, *Clay Minerals*, **29**, 105–113 (1994).

[14] T. Karbowiak, M. A. Saada, S. Rigolet, A. Ballandras, G. Weber, I. Bezverkhyy, M. Soulard, J. Patarin, J.-P. Bellat, New insights in the formation of silanol defects in silicalite-1 by water intrusion under high pressure, *Phys. Chem. Chem. Phys*., **12**, 11454–11466 (2010). DOI: 10.1039/c000931h

[15] C. Rosales-Landeros, C. E. Barrera-Díaz, B. Bilyeu, V. V. Guerrero, F. U. Núñez, A review on Cr(VI) adsorption using inorganic materials, *American Journal of Analytical Chemistry*, 4, 8–16 (2013). DOI: 10.4236/ajac.2013.47A002